On the early evolution of Local Group dwarf galaxy types: star formation and supernova feedback

Bermejo-Climent, José R ; Battaglia, Giuseppina ; Gallart, Carme ; Di Cintio, Arianna ; Brook, Chris B ; Cicuéndez, Luis ; Monelli, Matteo ; Leaman, Ryan ; Mayer, Lucio ; Peñarrubia, Jorge ; Read, Justin I

Abstract: According to star formation histories (SFHs), Local Group dwarf galaxies can be broadly classified in two types: those forming most of their stars before zz = 2 (fast) and those with more extended SFHs (slow). The most precise SFHs are usually derived from deep but not very spatially extended photometric data; this might alter the ratio of old to young stars when age gradients are present. Here, we correct for this effect and derive the mass formed in stars by zz = 2 for a sample of 16 Local Group dwarf galaxies. We explore early differences between fast and slow dwarfs, and evaluate the impact of internal feedback by supernovae (SNe) on the baryonic and dark matter (DM) component of the dwarfs. Fast dwarfs assembled more stellar mass at early times and have larger amounts of DM within the half-light radius than slow dwarfs. By imposing that slow dwarfs cannot have lost their gas by zz = 2, we constrain the maximum coupling efficiency of SN feedback to the gas and to the DM to be 10 per cent. We find that internal feedback alone appears insufficient to quench the SFH of fast dwarfs by gas deprivation, in particular for the fainter systems. Nonetheless, SN feedback can core the DM halo density profiles relatively easily, producing cores of the sizes of the half-light radius in fast dwarfs by zz = 2 with very low efficiencies. Amongst the 'classical' Milky Way satellites, we predict that the smallest cores should be found in Draco and Ursa Minor, while Sculptor and Fornax should host the largest ones.

DOI: https://doi.org/10.1093/mnras/sty1651

Originally published at:
Bermejo-Climent, José R; Battaglia, Giuseppina; Gallart, Carme; Di Cintio, Arianna; Brook, Chris B; Cicuéndez, Luis; Monelli, Matteo; Leaman, Ryan; Mayer, Lucio; Peñarrubia, Jorge; Read, Justin I (2018). On the early evolution of Local Group dwarf galaxy types: star formation and supernova feedback. Monthly Notices of the Royal Astronomical Society, 479(2):1514-1527.
DOI: https://doi.org/10.1093/mnras/sty1651

Monthly Notices
of the
ROYAL ASTRONOMICAL SOCIETY

MNRAS **479,** 1514–1527 (2018)
Advance Access publication 2018 June 26

doi:10.1093/mnras/sty1651

On the early evolution of Local Group dwarf galaxy types: star formation and supernova feedback

José R. Bermejo-Climent,[1,2,3,4★] Giuseppina Battaglia,[3,4★] Carme Gallart,[3,4] Arianna Di Cintio,[3,4,5] Chris B. Brook,[3,4] Luis Cicuéndez,[3,4] Matteo Monelli,[3,4] Ryan Leaman,[6] Lucio Mayer,[7] Jorge Peñarrubia[8] and Justin I. Read[9]

[1]*INAF/OAS Bologna, Via Piero Gobetti 101, Area della Ricerca CNR/INAF, I-40129 Bologna, Italy*
[2]*INFN, Sezione di Bologna, Via Irnerio 46, I-40126 Bologna, Italy*
[3]*Instituto de Astrofísica de Canarias, C/Via Lactea, s/n, E-38205 La Laguna, Tenerife, Spain*
[4]*Departamento de Astrofísica, Universidad de La Laguna, E-38206 La Laguna, Tenerife, Spain*
[5]*Leibniz Institute for Astrophysics Potsdam (AIP), An der Sternwarte 16, D-14482 Potsdam, Germany*
[6]*Max-Planck Institut für Astronomie, Königstuhl 17, D-69117 Heidelberg, Germany*
[7]*Center for Theoretical Astrophysics and Cosmology, Institute for Computational Science, University of Zurich, Winterthurerstrasse 190, CH-8057 Zurich, Switzerland*
[8]*Institute for Astronomy, University of Edinburgh, Blackford Hill, Edinburgh EH9 3HJ, UK*
[9]*Department of Physics, University of Surrey, Guildford GU2 7XH, UK*

Accepted 2018 June 20. Received 2018 June 15; in original form 2018 March 28

ABSTRACT

According to star formation histories (SFHs), Local Group dwarf galaxies can be broadly classified in two types: those forming most of their stars before $z = 2$ (*fast*) and those with more extended SFHs (*slow*). The most precise SFHs are usually derived from deep but not very spatially extended photometric data; this might alter the ratio of old to young stars when age gradients are present. Here, we correct for this effect and derive the mass formed in stars by $z = 2$ for a sample of 16 Local Group dwarf galaxies. We explore early differences between *fast* and *slow* dwarfs, and evaluate the impact of internal feedback by supernovae (SNe) on the baryonic and dark matter (DM) component of the dwarfs. *Fast* dwarfs assembled more stellar mass at early times and have larger amounts of DM within the half-light radius than *slow* dwarfs. By imposing that *slow* dwarfs cannot have lost their gas by $z = 2$, we constrain the maximum coupling efficiency of SN feedback to the gas and to the DM to be ∼10 per cent. We find that internal feedback alone appears insufficient to quench the SFH of *fast* dwarfs by gas deprivation, in particular for the fainter systems. Nonetheless, SN feedback can core the DM halo density profiles relatively easily, producing cores of the sizes of the half-light radius in *fast* dwarfs by $z = 2$ with very low efficiencies. Amongst the 'classical' Milky Way satellites, we predict that the smallest cores should be found in Draco and Ursa Minor, while Sculptor and Fornax should host the largest ones.

Key words: galaxies: dwarf – galaxies: evolution – galaxies: haloes – galaxies: star formation.

1 INTRODUCTION

Dwarf galaxies are the smallest and most numerous galaxies in the Universe. In the range of absolute magnitudes $M_V > -15$, they are typically classified into dwarf spheroidals (dSphs), gas-poor and passively evolving; dwarf irregulars (dIrrs), which are gas-rich and star-forming systems (e.g. Mateo 1998); and transition types (dTs) with intermediate properties between dSphs and dIrrs. The existence of different kinds of dwarf galaxies has opened a question that is still unsolved (Skillman & Bender 1995): Are the current properties of dwarf galaxies a result of their evolution or were they imprinted during their early assembly?

The star formation histories (SFHs) are an exquisite tool that allows us to reconstruct the lifetime evolution of galactic systems. Gallart et al. (2015) compared *accurate* literature SFHs for a sample of 18 Local Group (LG) dwarf galaxies, selecting only those derived from deep photometric data reaching down to below the oldest main-sequence turnoff (oMSTO), and established an alternative

★ E-mail: bermejo@iasfbo.inaf.it (JRBC); gbattaglia@iac.es (GB)

classification of dwarf galaxies based on their lifetime evolution: they were divided in *fast* dwarfs, those that formed the majority of their stellar component early on (before $z \simeq 2$), and *slow* dwarfs, that only formed a small fraction of their stars at early times and continued forming stars for almost a Hubble time. The proposed dichotomy is not equivalent to the commonly adopted, traditional one: all the *fast* dwarfs are dSphs or transition types; however, not all the *slow* types are dIrrs: e.g. Milky Way (MW) satellites such as the Carina, Fornax and Leo I dSphs can be classified as having *slow* SFHs.

In Gallart et al. (2015), the SFHs were normalized and compared in a relative way. However, many of these SFHs are derived from photometric data that are deep but do not cover the entire stellar component. This, and the presence of age gradients in the dwarfs' stellar population (e.g. Battaglia et al. 2006, 2012a,b; Hidalgo et al. 2013; del Pino, Aparicio & Hidalgo 2015) can result in an underestimation of the star formation at early times, since usually older stellar populations present more extended spatial distributions. Here, we extend the analysis by Gallart et al. (2015) correcting for the missing spatial coverage of the ancient stars for a similar sample of LG dwarf galaxies. This allows us to integrate the absolute amount of mass formed into stars up to $z \simeq 2$ ($\sim$10 Gyr ago) in order to learn more about possible early differences between *fast* and *slow* types. We focus on the stellar mass formed up to redshift $z = 2$ (>10 Gyr ago), $M_{\star,\,z>2}$, because at lower redshift the two types are already very distinct, in that most *fast* dwarfs have experienced no or very little star formation.

Much of the theoretical research about the evolution of dwarf galaxies focuses on answering how could dSphs have lost their gas. There have been proposed many environmental mechanisms for the gas removal, such as ram-pressure or tidal stripping by a massive central halo (Grebel, Gallagher & Harbeck 2003; Mayer et al. 2006; Mayer 2010, Gatto et al. 2013) and the effects of an ionizing cosmic UV background (Efstathiou 1992; Bullock et al. 2001; Salvadori & Ferrara 2009; Sawala et al. 2010). The importance of environmental effects is supported by the existence of the observed morphology–density relations in galaxy groups: dwarfs with different gas content are preferentially found in different environments, with dSphs usually inhabiting denser locations as the neighbourhood of a large galaxy like the MW or M31.

Another explored scenario for the gas removal is the internal feedback and the gas ejection through supernova-driven outflows (Dekel & Silk 1986; Mac Low & Ferrara 1999; Salvadori & Ferrara 2009; Sawala et al. 2010, among others). Our derivation of the stellar mass formed up to $z \simeq 2$ allows us to estimate the amount of energy injected by the supernovae (SNe) to the interstellar medium (ISM) up to this redshift, and to quantify if the stellar feedback is enough or not to remove the gas and quench the star formation on *fast* dwarfs at early times. This can be done by estimating the competing effect of the gravitational potential of the dark matter (DM) halo versus the SN energy injected. Since kinematic measurements can essentially determine the dynamical mass within the spatial extent of the kinematic tracer, we use abundance-matching (AM) relations to link the total DM halo mass to the stellar mass of each galaxy (e.g. Behroozi, Wechsler & Conroy 2013; Moster, Naab & White 2013; Brook et al. 2014).

The calculation of the amount of SN feedback in dwarf galaxies can also provide information about whether this energy could or not change the DM halo density profile of the different kinds of dwarfs. It has been proposed (Navarro, Eke & Frenk 1996a; Read & Gilmore 2005; Pontzen & Governato 2014) that the feedback energy coupled to the gas can subsequently modify the DM distribution by gravitational effects. This would solve the so-called 'cusp/core' problem, that is the mismatch between the observed mass profiles, consistent with homogeneous-density 'cores' (e.g. Flores & Primack 1994; Moore 1994; Kuzio de Naray, McGaugh & de Blok 2008; Battaglia et al. 2008; de Blok 2010; Walker & Peñarrubia 2011; Amorisco & Evans 2012) and the cosmological *N*-body simulations suggesting that if gravitational interactions between cold dark matter (CDM) particles dominate the structure formation, the DM density profiles are characterized by centrally divergent 'cusps' (Dubinski & Carlberg 1991; Navarro, Frenk & White 1996b).

A similar long-standing tension between observations of the nearby Universe and the standard cosmological model is the 'missing satellites' problem: ΛCDM simulations produce more DM haloes than observed galaxies, also in LG-like environments (Klypin et al. 1998; Moore et al. 1998). The mismatch can be explained with baryonic physics and likely involves SN feedback, an ionizing UV background, tidal stripping and possibly cusp-core transformations all working together in concert (e.g. Macciò et al. 2010; Zolotov et al. 2012; Wetzel et al. 2016; Sawala et al. 2016b); however, assuming a 'cuspy' NFW profile (Navarro, Frenk & White 1997), kinematic measurements suggest that the smallest galaxies would live in the smallest haloes, leaving some inhabited haloes that would not be small enough to prevent star formation, this is called the 'too big to fail' problem (Boylan-Kolchin, Bullock & Kaplinghat 2011; Garrison-Kimmel et al. 2014). The solution within the CDM paradigm to match these galaxies with larger DM haloes is the presence of cores that would explain the lower measured velocity dispersions (Brooks & Zolotov 2014; Brook & Di Cintio 2015a,b). The connection between 'cusp-core', 'too-big-to-fail' and AM relation was highlighted in Brook & Di Cintio (2015a): the authors used the dynamical mass at half-light radius for LG's dwarf galaxies to show that, when fitted by a mass-dependent cored profiles (Di Cintio et al. 2014), the kinematic of galaxies with $M_\star > 10^6\,\mathrm{M}_\odot$ is compatible with haloes more massive than $M_{\rm halo} \simeq 10^{10} M_\odot$, alleviating the 'too-big-to-fail' problem and providing a $M_\star - M_{\rm halo}$ relation in line with AM predictions.

Since the core creation can be explained with SN feedback (e.g. Peñarrubia et al. 2012; Di Cintio et al. 2014; Chan et al. 2015; Maxwell, Wadsley & Couchman 2015; Oñorbe et al. 2015; Tollet et al. 2016), here we quantify its capability to modify the DM halo profiles at early times, by $z = 2$, for our sample of dwarfs, by providing an observationally based accurate determination of the total mass in stars formed in stars by $z = 2$.

This paper is organized as follows: In Section 2, we detail the data sets and methodology used to correct the SFHs from the incomplete spatial sampling and obtain the mass formed into stars up to $z = 2$. In Section 3, we compare this derived quantity with present-day observables such as the stellar and dynamical mass as a function of the Gallart et al. (2015) dichotomy. In Section 4, we calculate the amount of SN feedback energy produced at early times (by $z = 2$) and study its capability to remove the gaseous component and to change the DM density profiles of our dwarfs. We summarize our results and conclusions in Section 5. In Appendix, we investigate the effect of allowing for the feedback energy to be all injected at even earlier times ($z = 6$), accounting for the expected lower DM halo masses; we compare our results to simulations and theoretical work in the literature and briefly make considerations on gas expulsion and core creation in fainter systems than those considered in the main text, such as ultrafaint dwarf (UFD) galaxies.

2 METHODOLOGY AND DATA SETS

One of our goals is to compare the amount of stellar mass formed at ancient times in LG dwarf galaxies, in order to identify possible differences in the early properties of *slow* and *fast* dwarfs. Our sample consists of 16 LG 'classical' dwarf galaxies.[1] 15 of them were drawn from the sample used in Gallart et al. (2015), from which we excluded the Large Magellanic Cloud, Small Magellanic Cloud, and IC1613, since the spatial properties of their most ancient stellar component are still largely undetermined. We have also added the Leo II dSph due to the recent availability of wide-area photometric catalogues (Stetson, private communication) and SFH (Monelli, private communication). A list of galaxies and their properties[2] is given in Table 1.

An important aspect to take into account when determining the amount of stellar mass formed at a given redshift is the existence of negative age gradients in several LG dwarf galaxies (e.g. Battaglia et al. 2006, 2012a,b; Hidalgo et al. 2013): for these small galaxies in general the old stars show a more spatially extended distribution than the younger ones. Since not all the LG dwarf galaxies benefit from SFHs derived from deep CMDs covering a large portion of the galaxy's stellar component, not correcting for the missing spatial coverage could result in underestimations of the stellar mass from SFH integration, in particular for the old, most spatially extended stellar populations.

It is possible to calculate the correction factor due to the missing spatial coverage by knowing the surface density profile and the structural parameters (ellipticity, position angle) of the spatial distribution of more than 10 Gyr old stars in each dwarf galaxy and the footprint of the data sets from which SFHs were derived. An accurate determination of the surface density profile and the structural parameters requires photometric data with a wide-area coverage. When available, we adopt the literature values derived from the radial distribution of stellar mass at lookback-times more than 10 Gyr ago from SFH determinations from very deep and spatially extended photometric data. In lack of such estimates, a suitable alternative for our goals is to use the horizontal branch (HB) as a tracer of more than 10 Gyr old stars, as supported by stellar evolutionary models. The HB is also about 3 mag brighter than the oMSTO; therefore, very wide-area photometric data reaching down to below the HB level are more much easily encountered in the literature/archives.

2.1 Spatial distribution of ancient stars

Table 1 lists the ellipticity, position angle θ[3], and scalelength of the exponential profile, $R_s^{\rm old}$, that we adopted for the greater than 10 Gyr old stellar component of each dwarf galaxy, together with the corresponding sources. As detailed below, the complete set of estimates was not available in the literature for all galaxies.

For And II, there was no estimate of the best-fitting exponential surface density profiles. Therefore, we use the Sérsic profile of index $n = 0.3$ by McConnachie, Arimoto & Irwin (2007).

For Draco, Ursa Minor, Carina, Leo I, and Leo II, we have estimated ourselves the best-fitting exponential surface density profile of the HB stars, and the corresponding structural parameters. To this aim, we use photometric catalogues of point-sources derived from archive data: CFHT/MegaCam for Draco and Ursa Minor (Irwin, private communication), CTIO/MOSAIC II for Carina (Battaglia et al. 2012b); compilations of data from different instruments for Leo I (Stetson et al. 2014) and Leo II (Stetson, private communication). We then isolate HB stars using a simple selection in magnitude and colour over the CMD.[4] A detailed explanation of the methodology for fitting the structural parameters and best-fitting surface (number) density profile can be found in Cicuéndez et al. (2018). Here, it suffices to say that the analysis is performed by applying Bayesian MCMC methods directly to the stars' position, following the formalism described in the appendix of Richardson et al. (2011); we apply the MCMC Hammer (Foreman-Mackey et al. 2013), a PYTHON implementation of the Affine Invariant MCMC Ensemble sampler (Goodman & Weare 2010). The dwarf galaxy's surface density profile is assumed to be an exponential profile; a constant term is added in order to account for contamination by fore/background sources. There are 7 free parameters in the fit: the central surface density (σ_0), exponential scalelength (R_s), central coordinates (α_0, δ_0), position angle (θ) and ellipticity (ϵ) of the dwarf galaxy's stellar component, and the surface density of contaminants (σ_c).

We compared our results with the spatial distribution parameters from McConnachie (2012) for the whole stellar population, finding always consistency with our results and the known presence or absence of population gradients in these systems (e.g. Battaglia et al. 2012b; Jin et al. 2016).

For And XVI and Aquarius there are no wide-area photometric catalogues reaching down to below the HB that we could access. Hence, for these two galaxies we use the half-light radius for the whole stellar component from McConnachie (2012), coupled with the transformation between scalelength and half-light radius by Wolf et al. (2010). This gives a lower limit on the scalelength of the old stars due to the possible presence of negative age gradients.

2.2 Star formation histories

The star formation rates (SFRs) as a function of cosmic time (i.e. SFHs) derived from deep CMDs are used to calculate the amount of mass formed more than 10 Gyr ago within the region probed by these deep photometric data sets. We summarize in Table 1 the sources of these data sets and the type of each dwarf galaxy according to the classification proposed by Gallart et al. (2015).

For the Fornax dSph, since the SFH by del Pino et al. (2013) comes from a very deep VLT/FORS photometric data set but with a tiny spatial coverage, we carry out our analysis also with the SFH from de Boer et al. (2012b), whose CTIO/Mosaic II data set is not as deep, but has a spatial sampling that is almost complete.

[1] Even though the distinction might be somewhat artificial, here we maintain the common nomenclature of 'classical' dwarf galaxies and 'ultrafaint' dwarf galaxies (UFDs) to refer broadly to LG dwarf galaxies whose existence was known prior and posterior to the advent of SDSS, respectively.

[2] We note that there are clear pieces of evidence that And II has experienced a relatively high-mass ratio merger (at least 1:10, see Amorisco, Evans & van de Ven 2014); this might have affected the observed properties of the stellar component of this system, such as its half-light ratio, and placed it out of dynamical equilibrium; at the same time, its observed SFH might be the mix of the SFHs from the two merging systems.

[3] Defined as the angle of the galaxy projected semimajor axis from North to East.

[4] Incompleteness due to crowding or different depths between pointings is not an issue given the low surface brightness of the galaxies we are examining and the relatively bright apparent magnitude of the HB relative to the depth of the photometric data sets.

Table 1. Structural parameters, derived parameters, and properties of the 16 analyzed dwarf galaxies: ellipticity, position angle, and 2D scalelength adopted for the old stellar component (ϵ, θ, $R_s^{\rm old}$), classification based on the SFH, coverage percentage, mass formed into stars up to $z = 2$ ($M_{\star,\,z>2}$), present-day luminosity in V band (L_V), mass-to-light ratio for the V band (M/L), heliocentric distance (d), line-of-sight velocity dispersion (σ_v), and 2D half-light radius of the overall stellar component ($R_{1/2}$).

Galaxy	ϵ	θ (°)	$R_s^{\rm old}$ (arcmin)	SFH	Coverage (%)	$M_{\star,\,z>2}$ (10^6 M$_\odot$)	L_V (10^6L$_\odot$)	M/L	d (kpc)	σ_v (km s^{-1})	$R_{1/2}$ (pc)
Cetus	0.33[2]	63[2]	0.98 ± 0.02[5]	fast[12]	$28.1^{+0.4}_{-0.5}$	$5.99^{+0.34}_{-0.34}$	2.60[2]	1.6[3]	790[32]	17 ± 2[2]	703 ± 31[2]
Tucana	0.48[2]	97[2]	0.54 ± 0.03[5]	fast[13]	$92.7^{+1.2}_{-1.3}$	$2.39^{+0.18}_{-0.14}$	0.56[2]	1.6[3]	899[33]	$15.8^{+4.1}_{-3.1}$ [2]	284 ± 54[2]
LGS-3	0.20[2]	0[2]	0.87 ± 0.09[5]	fast[14]	$59.5^{+4.1}_{-4.9}$	$1.57^{+0.32}_{-0.24}$	0.96[2]	1.0[3]	650[31]	$7.9^{+5.3}_{-2.9}$ [2]	470 ± 47[2]
Leo A	0.40[2]	114[2]	1.61 ± 0.68[8]	slow[15]	$42.0^{+25.0}_{-15.0}$	$0.66^{+0.91}_{-0.44}$	6.00[2]	0.5[3]	798[2]	9.3 ± 1.3[4]	354 ± 19[4]
And II	0.20[2]	34[2]	10.0 ± 8.5[11]	fast[16]	$5.0^{+58.0}_{-3.5}$	54^{+162}_{-50}	7.60[2]	1.0[3]	652[2]	7.3 ± 0.8[2]	1176 ± 50[2]
And XVI	0.00[2]	0[2]	0.53 ± 0.03[2]	slow[17]	$71.4^{+2.2}_{-2.1}$	$0.21^{+0.13}_{-0.07}$	0.41[2]	1.2[3]	525[2]	3.8 ± 2.9[4]	136 ± 15[2]
Draco	0.22[1]	82[1]	$5.41^{+0.31}_{-0.29}$ [1]	fast[18]	$90.8^{+1.3}_{-1.9}$	$0.56^{+0.15}_{-0.15}$	0.18[29]	1.8[3]	76[2]	9.1 ± 1.2[2]	221 ± 19[2]
UMi	0.52[1]	48[1]	$10.9^{+0.7}_{-0.6}$ [1]	fast[19]	$74.7^{+1.9}_{-2.4}$	$0.88^{+0.13}_{-0.11}$	0.29[2]	1.9[3]	76[2]	9.5 ± 1.1[2]	411 ± 31[2]
Sculptor	0.32[2]	99[2]	9.0 ± 0.3[7]	fast[20]	$99.3^{+0.2}_{-0.2}$	$6.78^{+0.60}_{-0.60}$	2.30[2]	1.7[3]	86[2]	9.2 ± 1.4[2]	283 ± 45[2]
Carina	0.28[1]	67[1]	$7.78^{+1.39}_{-1.15}$ [1]	slow[21]	$92.7^{+2.6}_{-4.5}$	$0.31^{+0.16}_{-0.14}$	0.38[2]	1.0[3]	105[2]	6.6 ± 1.2[2]	250 ± 39[2]
Phoenix	0.40[2]	5[2]	1.56 ± 0.05[6]	fast[22]	$37.0^{+0.9}_{-1.2}$	$2.40^{+0.25}_{-0.27}$	0.77[2]	1.8[3]	415[2]	9.3 ± 0.7[28]	274 ± 8[8]
Leo I	0.35[1]	77[1]	$2.35^{+0.09}_{-0.09}$ [1]	slow[23]	$13.1^{+0.9}_{-0.9}$	$0.39^{+0.28}_{-0.25}$	5.50[2]	0.9[3]	254[2]	9.2 ± 1.4[2]	251 ± 27[2]
Leo II	0.13[2]	12[2]	$1.99^{+0.15}_{-0.14}$ [1]	slow[24]	$13.9^{+2.1}_{-1.4}$	$0.77^{+0.28}_{-0.25}$	0.74[2]	1.6[3]	233[2]	6.6 ± 0.7[2]	176 ± 42[2]
Aquarius	0.50[2]	99[2]	0.88 ± 0.02[2]	slow[25]	$77.6^{+1.6}_{-1.5}$	$0.67^{+0.30}_{-0.31}$	1.60[2]	0.9[3]	1072[2]	$7.9^{+1.9}_{-1.6}$ [4]	458 ± 21[2]
Sextans	0.27[2]	52[2]	$12.7^{+0.4}_{-0.4}$ [9]	fast[26]	$51.4^{+1.9}_{-2.0}$	$3.21^{+1.02}_{-0.94}$	0.44[2]	1.6[3]	86[2]	7.9 ± 1.3[2]	695 ± 44[2]
Fornax	0.30[2]	41[2]	13.7 ± 0.2[10]	slow[27]	$2.2^{+0.1}_{-0.1}$	$18.9^{+4.8}_{-3.9}$	20.0[2]	1.2[3]	147[2]	11.7 ± 0.9[2]	710 ± 77[2]
				slow[30]	$88.2^{+0.5}_{-0.5}$	$3.8^{+0.8}_{-0.8}$					

Notes: [1]This work (MCMC Hammer) [2]McConnachie (2012) [3]Woo, Courteau & Dekel (2008) [4]Kirby et al. (2014) [5]Hidalgo et al. (2013) [6]Battaglia et al. (2012a) [7]Battaglia (2007) [8]Hidalgo private communication [9]Cicuéndez et al. (2018) [10]Battaglia et al. (2006) [11]McConnachie et al. (2007) [12]Monelli et al. (2010a) [13]Monelli et al. (2010b) [14]Hidalgo et al. (2011) [15]Cole et al. (2007) [16]Skillman et al. (2017) [17]Monelli et al. (2016) [18]Aparicio, Carrera & Martínez-Delgado (2001) [19]Carrera et al. (2002) [20]de Boer et al. (2012a) [21]de Boer et al. (2014) [22]Hidalgo et al. (2009) [23]Gallart et al. (1999) [24]Monelli private communication [25]Cole et al. (2014) [26]Lee et al. (2009) [27]del Pino et al. (2013) [28]Kacharov et al. (2017) [29]Irwin & Hatzidimitriou (1995) [30]de Boer et al. (2012b) [31]Bernard (2009) [32]Castellani, Marconi & Buonanno (1996) [33]Sarajedini et al. (2002).

2.3 Correction for the incomplete spatial sampling

We create mock galaxies following the surface density profile and structural parameters of the old stellar population (see Section 2.1 and Table 1). The procedure is based on the generation of 2D random arrays following the desired spatial distribution (see also appendix B of Cicuéndez et al. 2018).

We reproduce the spatial coverage of the observations from where the SFHs were derived, taking from the literature the size, shape, orientation, and deviation with respect to the dwarf central coordinates of the footprint of each photometric data set. Then, we define the *coverage* as the percentage of mock stars from the generated galaxies that fall into the limits of the observed footprint. We list in Table 1 the obtained coverage percentages, for which one can see a wide range of values: from very well covered galaxies, such as Sculptor, Tucana, or Carina, to observations that are missing the majority of the old stellar component, like the case of And II or Fornax for the del Pino et al. 2013 data set. It can be appreciated that the correction is non-negligible in several cases. The uncertainties in the coverage percentage were obtained by propagating the error in the scalelength of the old stellar population $R_s^{\rm old}$ and neglecting the errors in the ellipticity and the position angle, since the coverage determination is strongly dominated by $R_s^{\rm old}$.

As final step, we integrate the SFHs from the beginning of star formation to 10 Gyr ago ($z \simeq 2$). The resulting mass is then divided by the corresponding coverage percentage, and this yields the corrected mass formed into stars up to $z = 2$, $M_{\star,\,z>2}$. The uncertainties on $M_{\star,\,z>2}$ are calculated considering the intrinsic error of the SFRs and the error introduced by our procedure (i.e. the error in the coverage).

3 MASS FORMED INTO STARS UP TO $Z = 2$

In this section, we compare our derived value of $M_{\star,\,z>2}$ with present-day observables such as the stellar mass (Fig. 1) and the dynamical mass within the half-light radius (Fig. 2). We study the behaviour of these relations as a function of the *fast* and *slow* classification.

Due to the existence of age gradients, the relative fraction of old stellar population could have been underestimated in galaxies classified as *slow* in Gallart et al. (2015) and whose SFH was determined from data covering a small fraction of the main body. Thus, we first redefined a classification criterion based on our absolute quantities and checked whether our determination of $M_{\star,\,z>2}$ would result in a different classification than the one proposed by Gallart et al. (2015).

Ideally, one would want to use SFHs corrected for the missing spatial coverage for the whole lifetime of the galaxy. However, this would imply knowledge of the dependence of the scalelength of the spatial distribution of the stellar component as a function of age, which is not available. Instead, we calculate how much the old stellar component is contributing to the total present-day stellar mass. To this end, we use IAC-STAR (Aparicio & Gallart 2004) in order to calculate the fraction of $M_{\star,\,z>2}$ that remains alive to

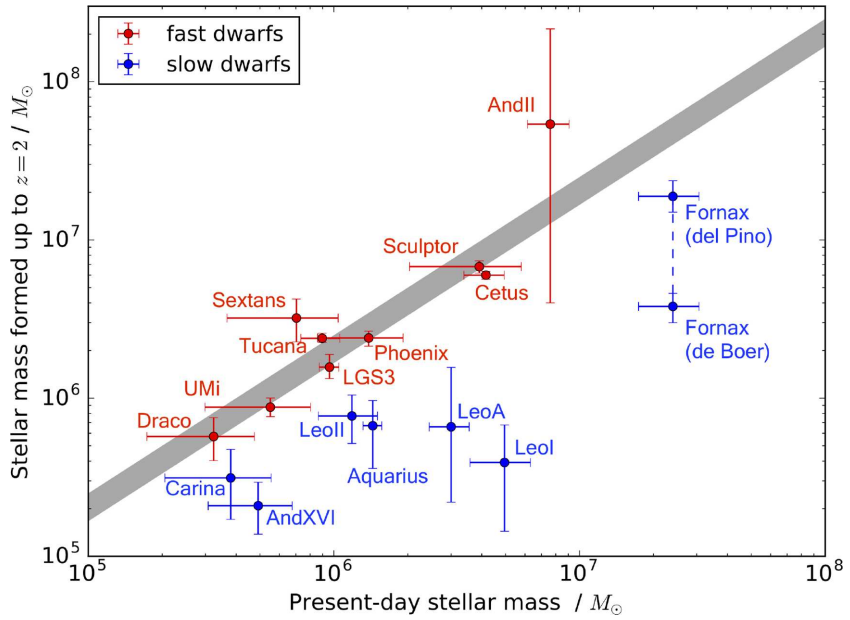

Figure 1. Stellar mass formed up to $z = 2$ ($M_{\star,\,z\,>\,2}$) as a function of the mass in stars still alive at the present-day ($M_\star^T$). The red and blue points represent respectively the *fast* and *slow* dwarfs according to the classification by Gallart et al. (2015). The x-axis errors are obtained propagating the uncertainties on M_V from McConnachie (2012). The y-axis errors are calculated considering the intrinsic error of the SFRs and the error introduced by our procedure (i.e. the error in the coverage). The grey band indicates the maximum $M_{\star,\,z\,>\,2}$ allowed as a function of present-day stellar mass, with the limits corresponding to this calculation done with remnants and without remnants once the effect of stellar evolution and death are taken into account.

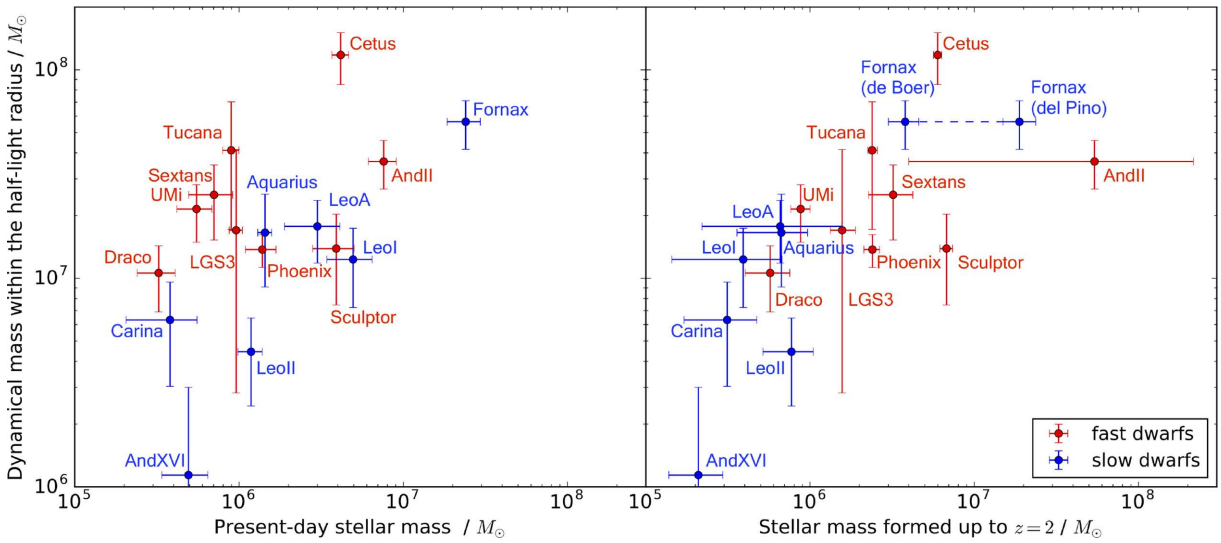

Figure 2. Dynamical mass within the half-light radius ($M_{\rm dyn}$) as a function of the present-day stellar mass ($M_\star^T$, left-hand panel) and stellar mass formed up to $z = 2$ ($M_{\star,\,z\,>\,2}$), right-hand panel). The red and blue points represent respectively the *fast* and *slow* dwarfs according to the classification by Gallart et al. (2015).

present-day, $M^{\rm alive}_{\star,z>2}$. By assuming a constant SFR between $t \simeq 13.5$ and $t = 10$ Gyr in lookback time and a typical metal-poor population, we obtain that ∼40 per cent of the mass formed in stars before 10 Gyr ago is still alive today (∼60 per cent when including remnants). Therefore, we adopt a 50 per cent factor to obtain $M^{\rm alive}_{\star,z>2}$. We checked that this number does not change specifically if the shape of the SFH at old times is different from constant, e.g. assuming it all concentrated within the first ∼1 Gyr. Then, we compare the obtained $M^{\rm alive}_{\star,z>2}$ with the present-day total stellar mass $M_\star^T$, that is derived using the luminosities from Table 1 and the stellar component mass-to-light ratios by Woo et al. (2008).[5] We define a dwarf galaxy as *fast* if $M^{\rm alive}_{\star,z>2} > (M_\star^T - M^{\rm alive}_{\star,z>2})$, i.e. when more than 50 per cent of its current mass in stars was formed before $z = 2$, or equivalently, when $M_{\star,z>2} > M_\star^T$. According to this criterion, all the analyzed galaxies remain of the same type as in Gallart et al. (2015). We note that Sextans falls off the permitted region in

[5]Woo et al. (2008) do not list *M*/*L* values for Cetus and And XVI. For those galaxies, we adopt the same *M*/*L* than for Tucana and Fornax (respectively) based on the similarity of their SFHs.

amount of ancient stars that could have formed given the present-day luminosity, but considering the errorbars, the discrepancy is not statistically significant.

3.1 Relation to the present-day stellar mass

In the work of Gallart et al. (2015), the life-time evolution of *fast* and *slow* dwarfs was compared in relative terms, using normalized SFHs. Fig. 1 shows that, when comparing galaxies at a similar present-day stellar mass, dwarfs classified as *fast* appear to have formed more stellar mass at ancient times than *slow* types, also in absolute terms. It could be argued that the above result may be intrinsic to the definition of *fast* and *slow* types; however, here we showed that the result holds also when correcting the amount of stellar mass formed at ancient times for the missing spatial coverage, which in several cases implied a significant correction. Furthermore, the trend of *fast* dwarfs being more massive at $z = 2$ than *slow* types appears to hold over about two orders of magnitude in current stellar mass. Information on the SFH of a system like WLM, of comparable stellar mass to Fornax but star forming and gas rich, would help in testing whether the trend continues at stellar masses above 10^7 $M_\odot$.

The values of $M_{\star,\,z>2}$ in And II and Fornax are the most uncertain, due to the very large error associated to $R_s^{\rm old}$ for the former and due to the different SFH determinations in the literature for the latter. Nonetheless, it is very likely that Fornax had the largest baryonic mass of the galaxies in the sample since early on, as it would be suggested by the fact that it contains five ancient globular clusters, while no GCs have been detected in And II, Sculptor and Cetus.

An additional interesting information provided by Fig. 1 is that all but one of the *slow* dwarfs in the sample formed a similarly low amount of stellar mass at early times ($2 \times 10^5 < M_\odot < 8 \times 10^5$), independently of their current stellar mass. Since these galaxies have all experienced star formation more recently than $z = 2$ and still contain gas at present, this may indicate that the SNe feedback associated with early stellar masses below 10^6 $M_\odot$ would be insufficient to induce a significant removal of gas and therefore would not result in an early quenching of the star formation.

On the other hand, the Milky Way satellites Draco and Ursa Minor have also formed similarly low stellar masses at ancient times but have had their star formation stopped by $z = 2$; we speculate then that star formation in these latter systems was not stopped by internal feedback alone (see also Section 4.2), but rather by other effects, such as ram-pressure stripping and/or reionization.

For example, Gallart et al. (2015) proposed that strong internal feedback and reionization may couple to induce important gas loss at early times leading to early quenching in *fast* dwarfs, while this coupling may not occur in slow dwarfs, in which the onset of star formation would be delayed and take place only when the DM halo has grown massive enough to allow the gas to cool and form stars after reionization. A similar dichotomy in SFHs was noticed in work by Benítez-Llambay et al. (2015), which makes use of the CLUES simulations (Gottloeber, Hoffman & Yepes 2010; Yepes, Gottlöber & Hoffman 2014). The dwarf galaxies with predominantly old SFHs are those inhabiting DM haloes that collapse early and where re-ionization coupled with internal feedback drives the low-density gas out of the virial radius, preventing further re-accretion: therefore, star formation continues only until the gas that had cooled down before re-ionization is eventually consumed. On the other hand, the dwarf galaxies with a predominantly young stellar population are inhabiting haloes that collapsed late and were thus unable to start forming stars in significant numbers until well after reionization. Several sets of simulations do lend support to the fact that the heating effect of internal feedback is enhanced by the UV background due to reionization (e.g. Sawala et al. 2010). Note that the effects of reionization could be spatially dependent, being stronger for those galaxies that were born closer to a growing source of reionization like the MW or M31 and affecting in a higher amount satellites like Draco and Ursa Minor (Miralda-Escudé, Haehnelt & Rees 2000; Weinmann et al. 2007; Spitler et al. 2012; Ocvirk et al. 2016; Dixon et al. 2018).

If Draco and Ursa Minor would have not been stripped of their gaseous component and been allowed to continue forming stars till present day, they might have turned out to be much more luminous, as their 'slower' Leo A, Leo I counterparts. Therefore, when exploring the hypothesis that passively evolving satellites of the MW and M31 shared similar ancestors as the gas-rich, star-forming isolated LG dwarfs, depending on the infall redshift of the satellite, one might have to compare systems of rather different present-day luminosity (see also Mistani et al. 2016 for similar conclusions between cluster and field dwarf galaxies).

3.2 Relation to the dynamical mass

Since at similar present-day stellar mass dwarf galaxies with a fast SFH appear to have formed a larger amount of stellar mass at early times than slow dwarfs, it is interesting to explore whether there are signs they could have assembled also more DM at early times.

To this aim, we consider the dynamical mass within the half-light radius ($M_{\rm dyn}$), which can be derived very accurately in pressure-supported spherical systems for which only line-of-sight velocities are available, such as the gas-poor dSphs, provided a few conditions are met (see Walker et al. 2009; Wolf et al. 2010). Many of the gas-rich LG dwarfs show little sign of rotation in their stellar component within their projected half-light radii (Leaman et al. 2012; Wheeler et al. 2017), therefore the same method has been applied to these systems too (e.g. Kirby et al. 2014).

Here, we use the formula by Walker et al. (2009):

$$M_{\rm dyn}[\,M_\odot] = 580 R_{1/2} \sigma_v^2, \qquad (1)$$

where $R_{1/2}$ is the 2D half-light radius in pc, σ_v is the line-of-sight velocity dispersion in km s^{-1}, for which we use the values referring to the overall stellar component (see Table 1). Since the LG dwarf galaxies we are analyzing are consistent with being DM dominated at all radii (see recent reviews by Battaglia, Helmi & Breddels 2013; Walker 2013 and references therein, although see Battaglia, Sollima & Nipoti 2015 and Diakogiannis et al. 2017 for the case of Fornax), $M_{\rm dyn}$ is essentially due to the mass of the DM halo within the half-light radius.[6] The effect of tidal stripping on to the DM haloes of satellite dwarf galaxies is to decrease the intrinsic σ_v (e.g. Read et al. 2006; Peñarrubia, Navarro & McConnachie 2008; Łokas, Kazantzidis & Mayer 2011; Kazantzidis et al. 2017) and to a less extent $R_{1/2}$ (Peñarrubia et al. 2008); therefore, the $M_{\rm dyn}$ value for satellite dwarf galaxies should be seen as a lower limit to the $M_{\rm dyn}$ before infall.

Fig. 2 shows that there are hints of a correlation between the present-day stellar mass and $M_{\rm dyn}$ (left-hand panel, see also McConnachie 2012); this correlation becomes better defined when considering the stellar mass formed at early times $M_{\star,\,z>2}$ (right-hand panel), rather than the present-day stellar mass. This is confirmed by a Pearson test, which yields a correlation coefficient equal

[6] We checked that the stellar mass within the half-light radius is negligible with respect to the total $M_{\rm dyn}$ in our dwarfs.

to 0.6 for $\log(M_{\rm dyn})$ versus $\log(M_\star^T)$ and 0.7 for $\log(M_{\rm dyn})$ versus $\log(M_{\star,\,z>2})$.

We speculate that the relation between $M_{\rm dyn}$ and $M_{\star,\,z>2}$ might be linking the DM and the baryonic content of these dwarf galaxies at early times, with $M_{\star,\,z>2}$ being a better tracer of the initial baryonic content than the present-day stellar mass. This is probably because, as discussed above, for systems that have had their evolution affected by external mechanisms, the present-day stellar mass is likely not representative of the stellar mass the system would have had if allowed to evolve in isolation.

We find that, in general, *fast* dwarfs have a larger DM content within the half-light radius with respect to *slow* dwarfs: excluding And II, which seems to be an outlier in terms of $R_{1/2}$, the median $M_{\rm dyn}$ is $1.9\times10^7\,{\rm M}_\odot$ for the *fast* ($2.2\times10^7\,{\rm M}_\odot$ if we do not exclude And II) and $1.2\times10^7\,{\rm M}_\odot$ for the *slow* dwarfs, respectively. This could, however, be a consequence of the larger $R_{1/2}$ found in *fast* dwarfs for the galaxies in our sample: the ratio between the median $R_{1/2}$ of both kind of dwarfs is ∼1.4 excluding And II (∼1.6 with And II), while the ratio between median dynamical masses is ∼1.5–1.6 (∼1.8 with And II). Given the relatively small size of our sample of galaxies, we cannot exclude that small number statistics might be affecting the result. Nonetheless we note that: (1) the DM mass for the *slow* dwarfs that are gas rich could be lower than estimated here, since we have neglected the contribution of the gas to $M_{\rm dyn}$; (2) the DM mass (and hence $M_{\rm dyn}$) for the dwarfs that are satellite galaxies, that is in general *fast* dwarfs, is expected to have been larger before infall, depending on the amount of tidal stripping undergone. These effects should, on average, go in the direction of emphasizing the difference in DM mass between *slow* and *fast* dwarfs.

4 SUPERNOVA FEEDBACK

We use our determination of the mass in stars formed up to $z=2$ to provide observationally motived estimates of the amount of stellar feedback from SNe explosions and comment on the possible effect that this might have had on the early evolution of the baryonic and DM component of LG dwarf galaxies. Specifically, we focus on the questions of whether the energy injected by SN is able to remove the gas and therefore halt star formation at early times in the *fast* dwarfs (Section 4.2) and/or to transform an initially cuspy DM halo into a cored one (Section 4.3).

We concentrate on SNe II because 3D hydrodynamical simulations show that the influence of the SNe Ia explosions on the general hydrodynamical behaviour of the ISM is not very important, due to the small percentage (∼3 per cent) of SNe Ia events during a cycle of SNe II explosions (e.g. Marcolini et al. 2006).

4.1 Derivation of SNe feedback energy and competing gravitational potential

In order to calculate the expected energy budget from SNe II explosions ($E_{{\rm SN},\,z=2}$), we assume that stars with masses $M\gtrsim6.5\,{\rm M}_\odot$ evolve into SNe II and calculate the expected numbers integrating the IMF by Kroupa (2001), given our estimates of $M_{\star,\,z>2}$. Considering a typical kinetic energy of 10^{51} erg for these kind of events (Utrobin & Chugai 2011), we obtain the total energy injected by SNe II in the environment up to $z\simeq2$. We list in Table 2 the values of $E_{{\rm SN},\,z=2}$. The choice of an SN II cut-off mass of $6.5\,{\rm M}_\odot$ was motivated by theoretical works (see e.g. Cassisi & Castellani 1993; Monelli et al. 2010b) predicting a lower value at the low metallicity of stellar populations in dwarf galaxies, with respect to the standard $8\pm1\,{\rm M}_\odot$ cut-off observed at solar, or higher, metallicity (see e.g. review by Smartt et al. 2009). We checked that the effect of choosing $M\gtrsim8\,{\rm M}_\odot$ as limit in mass for the integration does not change significantly the result: in that case, the feedback energy obtained is a ∼75 per cent of the $E_{{\rm SN},\,z=2}$ in the $M\gtrsim6.5\,{\rm M}_\odot$ case (see below for consequences on the results).

A key factor that strongly affects the analysis is the choice of what fraction of the energy produced by SN II couples to the gas and to the DM; this is parametrized through the so-called efficiency ($\epsilon_{\rm SN}$ and $\epsilon_{\rm DM}$). The value of this parameter is very uncertain, but as discussed for example in Peñarrubia et al. (2012), typical values are likely not to exceed $\epsilon_{\rm SN}=0.4$ (see e.g. Governato et al. 2010, whose simulations also include heating from the cosmic UV background) and might be as low as a few per cent ($\epsilon_{\rm SN}=0.01$, e.g. Kellermann 1989; in Revaz & Jablonka 2012 a value of $\epsilon_{\rm SN}=0.05$ best describes the metallicity–luminosity relation of MW dSphs). 3D hydrodynamical simulations of the chemical and dynamical evolution of the ISM in dwarf galaxies show that, in a picture where star formation proceeds in short bursts of 60 Myr, even if the energy released by SNe II in a *single* burst is about 1.3 times larger than the gas binding energy, no galactic wind develops due to the massive DM halo and the large effectiveness of the radiative losses (Marcolini et al. 2006); also in this case the SN efficiency appears to be ∼0.05. The range of efficiencies from observationally motivated works is compatible with the theoretical results, e.g. McQuinn et al. (2017) calculate an average wind efficiency of 0.16 for a burst time-scale of 25 Myr.

Another crucial ingredient to quantify the capability of the SNe feedback energy of removing the gas and/or modifying the DM halo density profile by $z=2$ is the competing effect of the gravitational potential W of the dwarf galaxy. As discussed above, LG dwarf galaxies are typically found to be DM dominated at all radii; therefore, we neglect the stellar component as a contributor to the gravitational potential (note that adding it would go in the direction of making gas removal or creation of cores in the DM halo more difficult). We assume a standard ΛCDM cosmology with $\Omega_{\rm m}=0.32$, $\Omega_\Lambda=0.68$, and $H_0=67\,{\rm km\,s^{-1}\,Mpc^{-1}}$ (e.g. Planck Collaboration XIII 2016).

The gravitational potential is defined as

$$W=-4\pi G\int_0^{R_{\rm vir}}\rho(r)M(r)r\,{\rm d}r, \tag{2}$$

where $\rho(r)$ is the DM halo density profile, $M(r)=\int_0^r\rho(r')4\pi r'^2{\rm d}r'$ and $R_{\rm vir}$ is the DM halo virial radius. The value of W at $z\simeq2$ is calculated as follows.

First, we obtain the DM halo mass at $z=0$ from the present-day stellar mass using the AM relation by Brook et al. (2014) based on LG simulations:

$$M_\star=\left(\frac{M_{\rm h}}{M_0\times10^6}\right)^{3.1}, \tag{3}$$

where $M_\star$ is the stellar mass, $M_{\rm h}$ is the halo mass and $M_0=79.6\,{\rm M}_\odot$. We also do the calculations using the AM relation from Moster et al. (2013):

$$\frac{M_\star}{M_{\rm h}}=2N\left[\left(\frac{M_{\rm h}}{M_1}\right)^{-\beta}+\left(\frac{M_{\rm h}}{M_1}\right)^{\gamma}\right]^{-1}, \tag{4}$$

where $M_1=11.59\,{\rm M}_\odot$, $N=0.0351$, $\beta=1.376$, and $\gamma=0.608$.

Secondly, we extrapolate the $z=0$ DM halo mass to $z\simeq2$ using the results by Fakhouri, Ma & Boylan-Kolchin (2010) (see their fig. 6), that for haloes in our regime of present-day mass

Table 2. Feedback and gravitational potential properties of the dwarfs at $z = 2$: budget of feedback energy (E_{SN}), virial mass of the DM halo ($M_{vir,\,z=2}$), gravitational potential of the DM halo ($W_{z=2}$) and minimum energy required to expel the gas ($\Delta W_{gas/2}$) and form a core of $r_c = R_{1/2}$ ($\Delta W_{core}/2$), calculated for both AM relations by B14 and M13.

Galaxy	E_{SN} (10^{54} erg)	$M_{vir,\,z=2}$ (10^9 M$_\odot$)		$W_{z=2}$ (10^{54} erg)		$\Delta W_{gas}/2$ (10^{54} erg)		$\Delta W_{core}/2$ (10^{54} erg)	
		B14	M13	B14	M13	B14	M13	B14	M13
Cetus	83	4.9	4.3	−60.8	−49.8	5.1	4.1	5.6	4.7
Tucana	33	3.0	2.3	−26.9	−17.2	2.2	1.4	1.4	1.0
LGS-3	22	3.0	2.3	−27.8	−18.0	2.3	1.5	2.2	1.5
Leo A	9	4.4	3.8	−51.1	−39.7	4.3	3.3	2.8	2.3
And II	748	5.9	5.6	−83.8	−75.7	7.0	6.3	9.5	9.8
And XVI	3	2.5	1.8	−19.5	−11.2	1.6	0.9	0.6	0.4
Draco	8	2.1	1.5	−15.5	−8.4	1.3	0.7	0.7	0.4
UMi	12	2.6	1.9	−20.7	−12.2	1.7	1.0	1.6	1.0
Sculptor	94	4.8	4.2	−58.8	−47.7	4.9	4.0	2.6	2.2
Carina	4	2.3	1.6	−17.0	−9.4	1.4	0.8	0.9	0.5
Phoenix	33	3.4	2.7	−33.9	−23.2	2.8	1.9	1.6	1.2
Leo I	5	5.2	4.7	−66.7	−56.2	5.6	4.7	2.6	2.3
Leo II	11	3.3	2.6	−31.1	−20.7	2.6	1.7	1.0	0.8
Aquarius	9	3.5	2.8	−34.5	−23.8	2.9	2.0	2.5	1.9
Sextans	45	2.8	2.1	−23.6	−14.5	2.0	1.2	2.5	1.7
Fornax (del Pino)	261	8.6	9.1	−154.8	f-168.7	12.9	14.0	1.2	1.3
Fornax (de Boer)	53	8.6	9.1	−154.8	−168.7	12.9	14.0	1.2	1.3

($\sim 10^{9-10}$ M$_\odot$) estimates the virial mass M_{vir} at $z = 2$ to be about 40–50 per cent of the current one (we have assumed $M_{vir} \simeq M_{halo}$).

Then, we obtain $R_{vir}(z = 2)$ from $M_{vir}(z = 2)$ following the formula[7]:

$$M_{vir}(z) = \frac{4\pi}{3}\Delta_{vir}(z)\rho_c R_{vir}^3(z). \quad (5)$$

For the density profile $\rho(r)$, we assume a Navarro-Frenk-White (NFW) profile (Navarro et al. 1997):

$$\rho_{NFW}(r) = \frac{\rho_s}{(r/r_s)(1 + r/r_s)^2}, \quad (6)$$

where to obtain the parameters ρ_s and r_s of the NFW profile it is useful to consider the concentration parameter $c_{vir} \equiv R_{vir}/r_s$. We calculate the concentration from $M_{vir}(z = 2)$ using the formula by Dutton & Macciò (2014):

$$\log_{10} c_{vir} = a + b \log_{10}(M_{vir}/[10^{12} h^{-1}\,\mathrm{M}_\odot]) \quad (7)$$

with $a = 0.643$ and $b = -0.051$ for $z = 2$. Thus, r_s is trivially obtained from R_{vir} and for ρ_s by applying the relation in Bullock et al. (2001):

$$M_{vir} = 4\pi\rho_s r_s^3 A(c_{vir}), \quad (8)$$

where $A(c_{vir})$ is defined as

$$A(c_{vir}) \equiv \log(1 + c_{vir}) - \frac{c_{vir}}{1 + c_{vir}}. \quad (9)$$

We decided not to use AM relations computed at $z = 2$ in order to get our stellar to halo mass, because the relation is poorly constrained at such redshift for halo masses below 10^{11}–10^{12} M$_\odot$. To check that our results do not depend strongly on the AM relation choice, we use both the Brook et al. (2014) AM relation (hereafter B14), which is based on LG simulations and observations, and the Moster et al. (2013) AM relation (hereafter M13) extrapolated to low-mass galaxies. We list in Table 2 the virial masses at $z = 2$ and gravitational potentials obtained for both AM relations. In Appendix, we comment on the effect of adopting the Behroozi et al. (2013) AM relation, which is the one that differs the most from the two above.

Note that the use of AM relations for dwarf galaxies that are satellites results in an upper limit for their halo mass, as we derive the pre-infall halo masses, while the masses at $z = 0$ could be much lower due the tidal stripping occurring after infall.

Simulations suggest that star formation proceeds in an oscillatory fashion, with 50–100 Myr long bursts, followed by similarly long quiescent periods, and that the impulsive heating due to this behaviour accumulates with time, eventually causing the transformation from a DM cusp into a core (e.g. Governato et al. 2010; Teyssier et al. 2013; Di Cintio et al. 2014), depending on the energy balance. As we will show in the Appendix, the results from our energetics calculations are in very good agreement with those from hydrodynamical simulations of dwarf galaxy formation by Read, Agertz & Collins (2016) when comparing the similar levels of energetics involved.

4.2 Early gas removal

Can the energy generated by the explosions of SNe II occurring at early times ($z > 2$) be the main driver for removing the gas in some of the LG dwarf galaxies? Can it explain the lack of star formation in *fast* dwarfs at times more recent than 10 Gyr ago?

To this end we consider the minimum energy required to expel the gas from the galaxy potential well as $\Delta W_{gas}/2 = (W_f - W_i)/2$, where the initial gravitational potential W_i is given by the sum of the DM halo gravitational potential and of the gas component, integrated out to the DM halo virial radius; while the final gravitational potential W_f is given only by the DM component, since the gas has been blown out. We also make the simplifying assumption that the density distribution of the gas follows an NFW profile as the DM halo and that the initial mass in gas is equal to the cosmological baryon fraction ($f_b \simeq 1/6$) times the DM halo mass. Given the uncertainties

[7]Here, ρ_c is the critical density of the Universe and Δ_{vir} is the virial overdensity, that for a flat cosmology can be approximated by (Bryan & Norman 1998): $\Delta_{vir}(z) \simeq \frac{18\pi^2 + 82x - 39x^2}{\Omega_m(z)}$, with $x = \Omega_m(z) - 1$, being $\Omega_m(z)$ the normalized matter density, whose redshift evolution is related to the present-day matter density Ω_m by the following formula: $\Omega_m(z) = \Omega_m \frac{(1+z)^3}{1-\Omega_m+(1+z)^3\Omega_m}$.

in the initial amount of gas present in these systems, this appears as a reasonable first-order approximation.

We start by considering the limiting case that all the energy-produced couples to the gas ($\epsilon_{\rm SN} = 1$), which can be interpreted as a strong upper limit on the capability of internal feedback to remove gas at early times. In this case, we find that practically all the systems (except maybe And XVI) would produce feedback energy in large enough amount as to remove the gaseous component. This is not realistic since in our sample there are galaxies with extended SFHs, indicating that the actual efficiency is less than 1.

We can constrain $\epsilon_{\rm SN}$ using the fact that *slow* dwarfs must have hold on to their gaseous component more recently than $z = 2$, to explain their extended SFHs. In particular, Fornax has a sizeable intermediate-age (1–8 Gyr old) component and has formed stars until very recently, ∼50–100 Myr ago (Coleman & de Jong 2008), suggesting that it must have retained a large fraction of its gas more recently than 10 Gyr ago. For this dwarf, $\epsilon_{\rm SN}$ cannot be higher than 10 per cent in order to retain the gas. Phoenix and LGS 3, which are both *fast* dwarfs but that still have some gas at present and have had some star formation after $z = 2$ (Hidalgo et al. 2009), would limit the efficiency to $\epsilon_{\rm SN} \lesssim 10$ per cent.

If we therefore assume $\epsilon_{\rm SN} \lesssim 10$ per cent, we obtain that the most luminous *fast* dwarfs (And II, Cetus, Tucana, Sculptor, and Sextans) could have been deprived of their gaseous component by stellar feedback. Under our hypotheses, it is natural to expect the systems that have produced the largest $M_{\star,\,z>2}$ to have a positive balance between $E_{\rm SN,\,gas,\,z=2}$ and the gravitational potential: while the energy produced by SNe II depends linearly on the stellar mass formed up to $z \simeq 2$, the gravitational potential depends ultimately on the halo mass, which according to Table 2 is rather similar ($\sim 10^{9-10}$ M$_\odot$) for the systems in our range of stellar masses.

Draco and Ursa Minor, which are found well within the virial radius of the MW and have stopped forming stars by $z = 2$, would need $\epsilon_{\rm SN} \simeq 15$ per cent to have had their star formation quenched by stellar feedback. If, as discussed above, $\epsilon_{\rm SN}$ is likely to be lower, these simple calculations would support the possibility discussed in the previous section that other factors, like tidal and/or ram-pressure stripping from the MW and re-ionization, can either be mainly responsible for the quenching of these two galaxies, or couple to internal feedback to make gas removal easier (see also Tomozeiu, Mayer & Quinn 2016a; Tomozeiu, Mayer & Quinn 2016b; Kazantzidis et al. 2017). On the other hand, should the DM halo masses of these galaxies be lower (as e.g. predicted by revised AM relations that correct for reduced stellar mass due to quenching, e.g. Read et al. in preparation), the capability of internal feedback to remove the gas would be enhanced.

However, in this approximation we are considering that all the energy produced by the SN II events occurring prior to $z = 2$ is injected at once in the ISM. Simulations suggest that star formation proceeds in an oscillatory way, with 50–100 Myr long bursts, followed by similarly long quiescent periods (Marcolini et al. 2006; Revaz et al. 2009). Part of the gas heated in a single short burst will cool down and fall back, to form the next generation of stars. So likely the net effect will be milder than what we are considering here. Clearly, the results concerning each specific galaxy should be taken with a grain of salt, but in general the comparison of the SNe energy budget with the gravitational potential at $z = 2$ indicates that internal feedback alone might not have been sufficient to deprive *fast* dwarf galaxies from their gas component at early times, under reasonable conditions of efficiency.

Even though we deem this hypothesis unlikely for the 'classical' dwarf galaxies, as those in our sample, in the Appendix we explore the impact of assuming that all the early star formation would occur by $z = 6$, rather than $z = 2$; we also make some consideration on feedback-driven gas loss in fainter systems than those considered here, such as those typically named as UFD galaxies.

4.3 Cuspy to cored profiles

We explore the possibility that the early SN feedback would produce changes in the DM halo density profile of the dwarf galaxies. It has been discussed, e.g. in Peñarrubia et al. (2012), that the transformation from cuspy, NFW profiles to cored profiles requires such an amount of energy that can only be generated by SNe II explosions. We follow these authors' formalism and consider the 3D mass density of the DM halo to follow the profile:

$$\rho_{\rm c}(r) = \frac{\rho_s r_s^3}{(r_{\rm c} + r)(r_s + r)^2}, \tag{10}$$

where $r_{\rm c}$ is the core radius, and r_s and ρ_s are the characteristic inner radius and density of the NFW profile. It can be shown that equation (10) reduces to the NFW profile described by equation (6) when $r_{\rm c} = 0$. According to Peñarrubia et al. (2012), and based on the virial theorem, the minimum energy required to core a profile is given by $\Delta W_{\rm core}/2 = (W_{\rm core} - W_{\rm cusp})/2$, where $W_{\rm core}$ is the gravitational potential of the cored DM halo, while $W_{\rm cusp}$ of the initially cusped DM halo.

Given that the gravitational potential of the cored profile depends on the core radius, we calculate the minimum energy to core the profile, $\Delta W_{\rm core}/2$, as a function of the core radius $r_{\rm c}$. In Table 2, we list the value of $\Delta W_{\rm core}/2$ for creating a core of equal size to the 2D half-light radius of each galaxy ($r_{\rm c} = R_{1/2}$). Fig. 3 shows the expected limits on the core radius that the galaxies in our sample can form using the energy from the SNe feedback due to $M_{\star,\,z>2}$ for the efficiency limits of $\epsilon_{\rm DM} = 0.01$ (leftmost cap in the figure) and $\epsilon_{\rm DM} = 0.40$ (rightmost cap in the figure) and assuming the B14 AM relation; the results for the M13 AM relation are extremely similar.

For each given galaxy, the results are heavily dependent on the choice for $\epsilon_{\rm DM}$ as there can be up to two orders of magnitude difference between the values of core radius obtained with $\epsilon_{\rm DM} = 0.01$ and 0.40 (our choice of 6.5 M$_\odot$ as the mass limit to form an SN II has a smaller effect on the results; increasing this to 8 M$_\odot$ results in cores with a 60–70 per cent smaller $r_{\rm c}$). This clearly highlights the need for more constrained estimates of the efficiency parameter.

If the main mechanism for core formation is the response of the DM halo to the change of gravitational potential induced by repeated short bursts of star formation, as suggested by simulations (e.g. Read & Gilmore 2005; Pontzen & Governato 2014), then the amount of SN II energy that radiates away does not contribute to this process, and therefore $\epsilon_{\rm DM}$ cannot be larger than $\epsilon_{\rm SN}$. If we consider the constraints on the efficiency discussed in Section 4.2, then we obtain $\epsilon_{\rm DM} \lesssim 10$–15 per cent.

For both the B14 and M13 AM relations, the galaxies with the largest $M_{\star,\,z>2}$ produce $r_{\rm c} > 5$ kpc already with an efficiency of $\epsilon_{\rm DM} \sim 0.1$–0.2. Observationally, there is an on-going debate as to whether MW satellites of the type considered here inhabit cuspy or cored DM haloes (e.g. Goerdt et al. 2006; Battaglia et al. 2008; Walker & Peñarrubia 2011; Agnello & Evans 2012; Cole et al. 2012; Jardel & Gebhardt 2013; Breddels & Helmi 2014; Richardson & Fairbairn 2014; Strigari, Frenk & White 2014). The observed kinematic (and light distribution) properties of the stellar component – and globular cluster system, for Fornax – are consistent with core sizes of ∼0.5–2 kpc. The upper limit on the core size is typically difficult to constrain (see e.g. Peñarrubia et al. 2012); however,

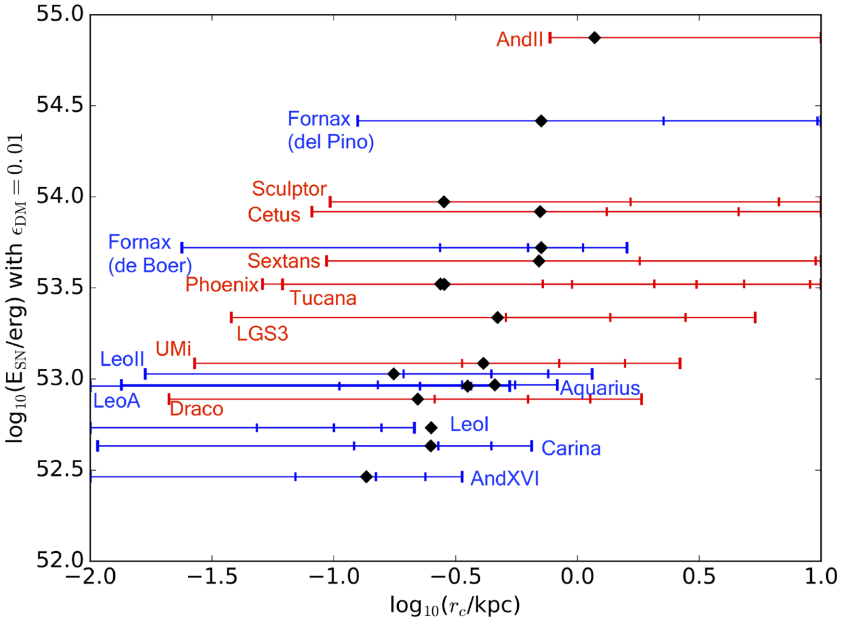

Figure 3. Expected limits on the core radius at $z = 2$ for the 16 dwarfs analyzed in this work assuming the AM relation from B14. The red and blue segments represent the fast and slow dwarfs, respectively. The outer caps of the segments correspond to efficiencies of $\epsilon_{\rm DM} = 0.01$ (left) and $\epsilon_{\rm DM} = 0.40$ (right), and the inner caps to $\epsilon_{\rm DM} = 0.1$, $\epsilon_{\rm DM} = 0.2$ and $\epsilon_{\rm DM} = 0.3$. The black diamonds correspond to the 2D half-light radii $R_{1/2}$ of each galaxy.

Amorisco & Evans (2012) exploited the presence of three stellar components among the Fornax red giant branch stars to limit the core size[8] of Fornax DM halo to $1.0^{+0.8}_{-0.4}$ kpc. In this respect, core sizes $r_{\rm c} > 5$ kpc can be considered as unlikely to be realistic, and this would be telling us that the $\epsilon_{\rm DM}$ ought to be less than 0.2. This is compatible with the constraints on the efficiency we provide in Section 4.2.

Except for Fornax when using the SFH from del Pino et al. (2013), all the *slow* dwarfs should have difficulties to form a core of $r_{\rm c} \gtrsim 1$ kpc given the conditions at $z = 2$ and would need a larger $\epsilon_{\rm DM}$ than what we constrain here to be able to produce core radii as large as their half-light radius by $z = 2$. On the other hand, the *fast* dwarfs have on average larger $M_{\star,\,z>2}$ and corresponding injection of energy into the ISM: in the regime of $\epsilon_{\rm DM} \lesssim 0.1$, the *fast* dwarfs appear to be able to form a core of $r_{\rm c} \sim R_{1/2}$ by $z = 2$, unless the efficiency is of only a few per cent. This could suggest that cuspy profiles (or the smallest cores) should be found preferentially in *slow* dwarfs, and it is in agreement with previous results from the analysis of Brook & Di Cintio (2015a) (see their fig. 7). In their work, two additional dwarfs are expected to be cuspy, namely Draco and UMi. They are the only two *fast* dwarfs in our scheme that form less than 10^6 $M_\odot$ in stars before $z = 2$, making the creation of a large core more difficult.

In our calculations, however, we are focusing on the energy budget at $z \sim 2$, ignoring stellar feedback from subsequent star formation. Hydrodynamical simulations by Read et al. (2016) and Di Cintio et al. (2017) show that cores with sizes comparable to the 3D half-light radius[9] of the stellar component can eventually form if star formation proceeds long enough (depending on the DM halo mass versus energy that couples to the DM). Subsequent star formation would have to compete against a growing DM halo, which might slow down the increase in core size, an effect that cannot be estimated in the simulations by Read et al. (2016) since the DM halo of their simulated dwarfs is not growing in time; however, it is probably safe to consider the core sizes of *slow* dwarfs as lower limits. On the other hand, the SF of *fast* dwarfs is either completely halted by $z = 2$ or just had some small residual activities; therefore, we do not expect an additional growth of the DM halo core size due to this effect.

As discussed by Maxwell et al. (2015), the Peñarrubia et al. (2012) approach has built in the assumption that the DM mass from the innermost regions can be redistributed by the feedback all the way to the DM halo virial radius. This leads to a larger amount of energy with respect to the one required to redistribute the DM halo mass within the region of the core, making core formation more difficult. The Peñarrubia et al. (2012) and Maxwell et al. (2015) approaches agree in the regime of 2–4 kpc core radii for DM halo masses in the range considered here. On the other hand, for smaller core radii, the estimates we are providing with the Peñarrubia et al. (2012) approach should be regarded as lower limits. Therefore, the formation of cores via internal feedback appears to be energetically feasible in the range of stellar and halo masses here considered.

We note that the B14 and M13 AM relations produce among the largest values of DM halo masses associated to dwarf galaxies of a given luminosity, which for the dwarf galaxies here analyzed range between $1.5 - 10 \times 10^9$ $M_\odot$ at $z = 2$. If we evolve back to $z = 2$, the DM halo masses predicted for the AM relation by Behroozi et al. (2013), which is the most different from the previous two, the DM halo masses would be much smaller, ranging from $\sim 1.5 \times 10^8$ $M_\odot$ to $\sim 3 \times 10^9$ $M_\odot$, yielding even larger core radii (see Appendix).

Given the exquisite spectroscopic data sets of several hundreds, or even thousands, accurate line of sight velocities of individual stars existing for the bright early-type galaxies satellites of the Milky Way (e.g. see review articles Battaglia et al. 2013; Walker 2013), the exciting recent measurement of the internal transverse motion of one of them (Massari et al. 2017), and the progress in

[8] We note that the authors do not statistically exclude a cuspy, NFW halo.
[9] Wolf et al. (2010) show that the 3D half-light radius is $\sim$1.3 the 2D half-light radius for a variety of commonly used surface density profiles.

sophisticated dynamical modelling tools (e.g. Breddels et al. 2013; Zhu et al. 2016; Read & Steger 2017), MW satellite galaxies are the LG dwarfs for which we can aim to have the best DM halo properties determinations. Among the MW satellites in our sample, those expected to have still a cusp or the smallest cores are Draco and Ursa Minor, while the largest ones are likely to be found in Sculptor and Fornax.

Note that Laporte & Peñarrubia (2015) discuss that the accretion of dark haloes can result into a cusp regrowth; however, it is unclear on which timescales and what environments this process is more likely to occur.

5 SUMMARY AND CONCLUSIONS

In this paper, we have performed an observationally motivated analysis of the early evolution of 16 LG dwarf galaxies, using accurate SFHs from the literature. We follow the classification in *fast* and *slow* dwarfs proposed by Gallart et al. (2015) and study whether their different present-day properties and life-time evolution can be traced back to differences in the early properties of these two main galaxy types.

Since the SFHs of our sample of dwarfs are usually derived from photometric data sets that cover only a fraction of the dwarfs' stellar component, we correct for the incomplete spatial sampling using statistical tools. To this end, we create mock galaxies following the surface density profile and structural parameters of the ancient stars ($>$ 10Gyr old, i.e. formed prior to $z = 2$) stars. The information on the spatial properties of the ancient stars is obtained either from the literature, when available, or by our own MCMC analysis of HB stars selected from wide-area photometric catalogues. We integrate the SFHs up to $z = 2$ ($\sim$10 Gyr ago) and correct the resulting formed stellar mass for the missing coverage. Our correction is found to be non-negligible in the majority of the cases.

We find that *fast* dwarfs formed more stellar mass by $z = 2$ than *slow* types over the two orders of magnitude probed by the data. This result adds information in absolute terms that was missing in the relative comparison by Gallart et al. (2015). The availability of more SFHs in the literature for dwarfs of larger stellar mass, like WLM, could confirm if this trend holds also at present-day stellar masses $> 10^7$ M$_\odot$. Additionally, we find hints that the DM haloes of *fast* dwarfs have on average a larger dynamical mass than those of *slow types* within the half-light radius. We also find a correlation between the dwarfs' dynamical mass within the half-light radius and the amount of stars formed by $z = 2$, which is clearer than when considering instead their present-day luminosity; we interpret this as $M_{\star,z>2}$ being a better indicator of the initial relative baryonic content of the galaxies in the sample, before environmental effects might have deprived some of them of their gaseous component (and prevented subsequent growth in stellar mass).

Our estimation of the stellar mass formed up to $z = 2$ is also useful to explore if stellar feedback could have removed the gas component of the *fast* dwarfs and to what extent it might have caused a transformation from a cuspy to cored DM halo. As expected, a key, but unknown, parameter in this kind of estimates is the efficiency with which the SN energy couples to the gas and DM. By requiring that dwarfs that have experienced significant star formation more recently than $z = 2$ cannot have been deprived of their gaseous component at ancient times, we are able to put limits on the possible amount of gas coupling efficiency, and consequently on the capability of feedback to halt star formation in *fast* dwarfs and to core DM profiles. Our limits are compatible with the observational constraints on the core radius estimates for the Fornax dwarf galaxy.

We find that the gas removal by $z = 2$ driven only by internal feedback would be possible in the *fast* dwarf galaxies with a massive stellar component, under reasonable conditions of efficiency according to our limits ($\epsilon_{\rm SN} \lesssim$ 10–15 per cent). Our analysis however assumes that all the SN II energy is injected at once, rather than in short bursts followed by quiescent periods, which might overestimate the capability of the feedback to expel the gas. Therefore, it is more likely that internal feedback alone cannot explain the quenching of star formation in *fast dwarfs*, in particular at the fainter end, and that other factors, such as ram/tidal-stripping and/or re-ionization might play a role too.

Regarding the 'cusp-core' problem, we find that the feedback energy would have been enough to produce a transformation from cuspy to cored profiles in most of the dwarf galaxies in the sample by $z = 2$. Our result is quite degenerated depending on the assumed feedback efficiency. This parameter is one of the most important quantities to be constrained in order to break the degeneracy with the core radius size. For the range of efficiencies that we can constrain using the fact that *slow* dwarfs cannot have removed their gaseous component, we find that *fast* dwarfs could have formed a core of size of the order of their 2D half-light radius ($r_{\rm c} \sim R_{1/2}$) by $z = 2$.

The DM core sizes we derive here should be considered as lower limits: we neglect the feedback after $z = 2$, which, if considered, would yield larger cores for the *slow* dwarfs; and as discussed in Section 4.3 the Peñarrubia et al. (2012) formalism has higher energy requirements for core formation with respect to the Maxwell et al. (2015) formalism. However, unless the SN II energy coupling to the DM is of only a few per cent, cores of at least 0.1–0.2 kpc appear to be energetically feasible to produce even within our conservative approach.

Among the MW satellites considered here, the systems that offer the best prospects for detecting a cusp (or where we expect the smaller cores to be) appear to be systems such as Draco and Ursa Minor, which also have *fast* SFHs and therefore do not suffer from the possibility of core size increase due to neglected SF $<$10 Gyr ago. At the opposite end sit Sculptor and Fornax (with the del Pino et al. 2013 SFH); in particular the latter, given its significant SF at intermediate ages, should be the system most likely to host a comparatively large core. We emphasize that the 'core-most' and 'cuspy-most' MW satellites are the same ones that were obtained with a different method in Brook & Di Cintio (2015a).

ACKNOWLEDGEMENTS

The authors are grateful to S. Hidalgo for providing the estimate of the half-light radius of the ancient component of Leo A, T. J. L. de Boer for the determination of the SFH of Fornax, P. Stetson and M. Irwin for kindly sharing reduced photometric catalogues and the anonymous referee for useful suggestions. JRBC gratefully acknowledges Instituto de Astrofísica de Canarias (IAC) for its hospitality and travel support during visits. GB gratefully acknowledges financial support by the Spanish Ministry of Economy and Competitiveness (MINECO) under the Ramon y Cajal Programme (RYC-2012-11537) and the grant AYA2014-56795-P; the latter grant supports also CG, MM, LC. ADC acknowledges financial support from a Marie-Sklodowska-Curie Individual Fellowship grant, H2020-MSCA-IF-2016 Grant agreement 748213, DIGESTIVO. JIR would like to acknowledge support from the STFC consolidated grant ST/M000990/1 and the MERAC foundation.

REFERENCES

Agnello A., Evans N. W., 2012, ApJ, 754, L39
Amorisco N. C., Evans N. W., 2012, MNRAS, 419, 184
Amorisco N. C., Evans N. W., van de Ven G., 2014, Nature, 507, 335
Aparicio A., Gallart C., 2004, AJ, 128, 1465
Aparicio A., Carrera R., Martínez-Delgado D., 2001, AJ, 122, 2524
Aparicio A. et al., 2016, ApJ, 823, 9
Battaglia G. et al., 2006, A&A, 459, 423
Battaglia G., 2007, PhD thesis, University of Gröningen
Battaglia G., Helmi A., Tolstoy E., Irwin M., Hill V., Jablonka P., 2008, ApJ, 681, L13
Battaglia G., Rejkuba M, Tolstoy E., Irwin M. J., Beccari G., 2012a, MNRAS, 424, 1113
Battaglia G., Irwin M. J., Tolstoy E., de Boer T. , Mateo M., 2012b, ApJ, 761, L31
Battaglia G., Helmi A., Breddels M., 2013, New A Rev., 57, 52
Battaglia G., Sollima A., Nipoti C., 2015, MNRAS, 454, 2401
Behroozi P. S., Wechsler R. H., Conroy C., 2013, ApJ, 770, 57
Benítez-Llambay A., Navarro J. F., Abadi M. G., Gottlöber S., Yepes G., Hoffman Y., Steinmetz M., 2015, MNRAS, 450, 4207
Bernard E. J., 2009, PhD thesis, University of La Laguna
Bovill M. S., Ricotti M., 2011, ApJ, 741, 17
Boylan-Kolchin M., Bullock J. S., Kaplinghat M., 2011, MNRAS, 415, L40
Breddels M. A., Helmi A., 2014, ApJ, 791, L3
Breddels M. A., Helmi A., van den Bosch R. C. E., van de Ven G., Battaglia G., 2013, MNRAS, 433, 3173
Brook C. B., Di Cintio A., 2015a, MNRAS, 450, 3920
Brook C. B., Di Cintio A., 2015b, MNRAS, 453, 2133
Brook C. B., Di Cintio A., Knebe A., Gottlöber S., Hoffman Y., Yepes G., Garrison-Kimmel S., 2014, ApJ, 784, L14 (B14)
Brooks A. M., Zolotov A., 2014, ApJ, 786, 87
Brown T. M. et al., 2014, ApJ, 796, 91
Bryan G. L., Norman M. L., 1998, ApJ, 495, 80
Bullock J. S., Kolatt T. S., Sigad Y., Somerville R. S., Kravtsov A. V., Klypin A. A., Primack J. R., Dekel A., 2001, MNRAS, 321, 559
Carrera R., Aparicio A., Martínez-Delgado D., Alonso-García J., 2002, AJ, 123, 3199
Cassisi S., Castellani V., 1993, ApJS, 88, 509
Castellani M., Marconi G., Buonanno R., 1996, A&A, 310, 715
Chan T. K., Kereš D., Oñorbe J., Hopkins P. F., Muratov A. L., Faucher-Giguère C.-A., Quataert E., 2015, MNRAS, 454, 2981
Cicuéndez L. et al., 2018, A&A, 609, A53
Cole A. A. et al., 2007, ApJ, 659, L17
Cole D. R., Dehnen W., Read J. I., Wilkinson M. I., 2012, MNRAS, 426, 601
Cole A. A., Weisz D. R., Dolphin A. E., Skillman E. D., McConnachie A. W., Brooks A. M., Leaman R., 2014, ApJ, 795, 54
Coleman M. G., de Jong J. T. A., 2008, ApJ, 685, 933
de Blok W. J. G., 2010, Adv. Astron., 2010, 789293
de Boer T. J. L. et al., 2012a, A&A, 539, A103
de Boer T. J. L. et al., 2012b, A&A, 544, A73
de Boer T. J. L., Tolstoy E., Lemasle B., Saha A., Olszewski E. W., Mateo M., Irwin M. J., Battaglia G., 2014, A&A, 572, A10
Dekel A., Silk J., 1986, ApJ, 303, 39
del Pino A., Hidalgo S. L., Aparicio A., Gallart C., Carrera R., Monelli M., Buonanno R., Marconi G., 2013, MNRAS, 433, 1505
del Pino A., Aparicio A., Hidalgo S. L., 2015, MNRAS, 454, 3996
Di Cintio A., Brook C. B., Macciò A. V., Stinson G. S., Knebe A., Dutton A. A., Wadsley J., 2014, MNRAS, 437, 415
Di Cintio A., Brook C. B., Dutton A. A., Macciò A. V., Obreja A., Dekel A., 2017, MNRAS, 466, L1
Diakogiannis F. I., Lewis G. F., Ibata R. A., Guglielmo M., Kafle P. R., Wilkinson M. I., Power C., 2017, MNRAS, 470, 2034
Dixon K. L., Iliev I. T., Gottlöber S., Yepes G., Knebe A., Libeskind N., Hoffman Y., 2018, MNRAS, 477, 867
Dubinski J., Carlberg R. G., 1991, ApJ, 378, 496
Dutton A. A., Macciò A. V., 2014, MNRAS, 441, 3359
Efstathiou G., 1992, MNRAS, 256, 43p
Fakhouri O., Ma C.-P., Boylan-Kolchin M., 2010, MNRAS, 406, 2267
Flores R. A., Primack J. R., 1994, ApJ, 427, L1
Foreman-Mackey D., Hogg D. W., Lang D., Goodman J., 2013, PASP, 125, 306
Frebel A., Simon J. D., Kirby E. N., 2014, ApJ, 786, 74
Gallart C., Freedman W. L., Aparicio A., Bertelli G., Chiosi C., 1999, AJ, 118, 2245
Gallart C. et al., 2015, ApJ, 811, L18
Garrison-Kimmel S., Boylan-Kolchin M., Bullock J. S., Kirby E. N., 2014, MNRAS, 444, 222
Gatto A., Fraternali F., Read J. I., Marinacci F., Lux H., Walch S., 2013, MNRAS, 433, 2749
Goerdt T., Moore B., Read J. I., Stadel J., Zemp M., 2006, MNRAS, 368, 1073
Goodman J., Weare J., 2010, Commun. Appl. Math. Comput. Sci., 5, 65
Gottloeber S., Hoffman Y., Yepes G., 2010, preprint (arXiv:1005.2687)
Governato F. et al., 2010, Nature, 463, 203
Grebel E. K., Gallagher J. S., III, Harbeck D., 2003, AJ, 125, 1926
Hidalgo S. L. et al., 2011, ApJ, 730, 14
Hidalgo S. L. et al., 2013, ApJ, 778, 103
Hidalgo S. L., Aparicio A., Martínez-Delgado D., Gallart C., 2009, ApJ, 705, 704
Irwin M., Hatzidimitriou D., 1995, MNRAS, 277, 1354
Jardel J. R., Gebhardt K., 2013, ApJ, 775, L30
Jin S., Irwin M., Tolstoy E., Lewis J., Hartke J., 2016, in Skillen I., Barcells M., Trager S., eds, ASP Conf. Ser. Vol. 507, Multi-Object Spectroscopy in the Next Decade: Big Questions, Large Surveys, and Wide Fields. Astron. Soc. Pac., San Francisco, p. 241
Kacharov N. et al., 2017, MNRAS, 466, 2006
Kazantzidis S., Mayer L., Callegari S., Dotti M., Moustakas L. A., 2017, ApJ, 836, L13
Kellermann K. I., 1989, The Observatory, 109, 163
Kirby E. N., Bullock J. S., Boylan-Kolchin M., Kaplinghat M., Cohen J. G., 2014, MNRAS, 439, 1015
Klypin A. A., Kravtsov A. V., Colin P., Gottlober S., Khokhlov A. M., 1998, American Astronomical Society Meeting Abstracts. p. 1336
Kroupa P., 2001, MNRAS, 322, 231
Kuzio de Naray R., McGaugh S. S., de Blok W. J. G., 2008, ApJ, 676, 920
Laporte C. F. P., Peñarrubia J., 2015, MNRAS, 449, L90
Leaman R. et al., 2012, ApJ, 750, 33
Lee M. G., Yuk I.-S., Park H. S., Harris J., Zaritsky D., 2009, ApJ, 703, 692
Łokas E. L., Kazantzidis S., Mayer L., 2011, ApJ, 739, 46
Mac Low M.-M., Ferrara A., 1999, ApJ, 513, 142
Macciò A. V., Kang X., Fontanot F., Somerville R. S., Koposov S., Monaco P., 2010, MNRAS, 402, 1995
Marcolini A., D'Ercole A., Brighenti F., Recchi S., 2006, MNRAS, 371, 643
Massari D., Breddels M. A., Helmi A., Posti L., Brown A. G. A., Tolstoy E., 2017, Nat. Astron., 2, 156
Mateo M. L., 1998, ARA&A, 36, 435
Maxwell A. J., Wadsley J., Couchman H. M. P., 2015, ApJ, 806, 229
Mayer L., 2010, Adv. Astron., 2010, 278434
Mayer L., Mastropietro C., Wadsley J., Stadel J., Moore B., 2006, MNRAS, 369, 1021
McConnachie A. W., 2012, AJ, 144, 4
McConnachie A. W., Arimoto N., Irwin M., 2007, MNRAS, 379, 379
McQuinn K. B. W., Skillman E. D., Heliman T. N., Mitchell N. P., Kelley T., 2017, MNRAS, 477, 3164
Miralda-Escudé J., Haehnelt M., Rees M. J., 2000, ApJ, 530, 1
Mistani P. A. et al., 2016, MNRAS, 455, 2323
Monelli M. et al., 2010a, ApJ, 720, 1225
Monelli M. et al., 2010b, ApJ, 722, 1864
Monelli M. et al., 2016, ApJ, 819, 147
Moore B., 1994, Nature, 370, 629
Moore B., Governato F., Quinn T., Stadel J., Lake G., 1998, ApJ, 499, L5
Moster B. P., Naab T., White S. D. M., 2013, MNRAS, 428, 3121 (M13)
Navarro J. F., Eke V. R., Frenk C. S., 1996a, MNRAS, 283, L72

Navarro J. F., Frenk C. S., White S. D. M., 1996b, ApJ, 462, 563
Navarro J. F., Frenk C. S., White S. D. M., 1997, ApJ, 490, 493
Ocvirk P. et al., 2016, MNRAS, 463, 1462
Oñorbe J., Boylan-Kolchin M., Bullock J. S., Hopkins P. F., Kereš D., Faucher-Giguère C.-A., Quataert E., Murray N., 2015, MNRAS, 454, 2092
Peñarrubia J., Navarro J. F., McConnachie A. W., 2008, ApJ, 673, 226
Peñarrubia J., Pontzen A., Walker M. G., Koposov S. E., 2012, ApJ, 759, L42
Planck Collaboration XIII, 2016, A&A, 594, A13
Pontzen A., Governato F., 2014, Nature, 506, 171
Read J. I., Gilmore G., 2005, MNRAS, 356, 107
Read J. I., Steger P., 2017, MNRAS, 471, 4541
Read J. I., Wilkinson M. I., Evans N. W., Gilmore G., Kleyna J. T., 2006, MNRAS, 367, 387
Read J. I., Agertz O., Collins M. L. M., 2016, MNRAS, 459, 2573 (R16)
Revaz Y. et al., 2009, A&A, 501, 189
Revaz Y., Jablonka P., 2012, A&A, 538, A82
Revaz Y., Jablonka P., Teyssier R., Mayer L., 2016, Star Formation in Galaxy Evolution: Connecting Numerical Models to Reality, Saas-Fee Advanced Course, Volume 43. Springer-Verlag Berlin, Heidelberg
Richardson J. C. et al., 2011, ApJ, 732, 76
Richardson T., Fairbairn M., 2014, MNRAS, 441, 1584
Salvadori S., Ferrara A., 2009, MNRAS, 395, L6
Sarajedini A. et al., 2002, ApJ, 567, 915
Sawala T. et al., 2016a, MNRAS, 456, 85
Sawala T. et al., 2016b, MNRAS, 457, 1931
Sawala T., Scannapieco C., Maio U., White S., 2010, MNRAS, 402, 1599
Skillman E. D., Bender R., 1995, Rev. Mex. Astron. Astrofis. Ser. Conf., 3, 25
Skillman E. D. et al., 2017, ApJ, 837, 102
Smartt S. J., Eldridge J. J., Crockett R. M., Maund J. R., 2009, MNRAS, 395, 1409
Spitler L. R., Romanowsky A. J., Diemand J., Strader J., Forbes D. A., Moore B., Brodie J. P., 2012, MNRAS, 423, 2177
Stetson P. B., Fiorentino G., Bono G., Bernard E. J., Monelli M., Iannicola G., Gallart C., Ferraro I., 2014, PASP, 126, 616
Strigari L. E., Frenk C. S., White S. D. M., 2014, preprint (arXiv:1406.6079)
Teyssier R., Pontzen A., Dubois Y., Read J. I., 2013, MNRAS, 429, 3068
Tollet E. et al., 2016, MNRAS, 456, 3542
Tomozeiu M., Mayer L., Quinn T., 2016a, ApJ, 818, 193
Tomozeiu M., Mayer L., Quinn T., 2016b, ApJ, 827, L15
Utrobin V. P., Chugai N. N., 2011, A&A, 532, A100
Walker M., 2013, in Oswalt T. D., Gilmore G. eds, Dark Matter in the Galactic Dwarf Spheroidal Satellites. Springer, Dordrecht, p. 1039
Walker M. G., Peñarrubia J., 2011, ApJ, 742, 20
Walker M. G., Mateo M., Olszewski E. W., Peñarrubia J., Wyn Evans N., Gilmore G., 2009, ApJ, 704, 1274
Weinmann S. M., Macciò A. V., Iliev I. T., Mellema G., Moore B., 2007, MNRAS, 381, 367
Wetzel A. R., Hopkins P. F., Kim J.-h., Faucher-Giguère C.-A., Kereš D., Quataert E., 2016, ApJ, 827, L23
Wheeler C. et al., 2017, MNRAS, 465, 2420
Wolf J., Martinez G. D., Bullock J. S., Kaplinghat M., Geha M., Muñoz R. R., Simon J. D., Avedo F. F., 2010, MNRAS, 406, 1220
Woo J., Courteau S., Dekel A., 2008, MNRAS, 390, 1453
Yepes G., Gottlöber S., Hoffman Y., 2014, New A Rev., 58, 1
Zhu L., van de Ven G., Watkins L. L., Posti L., 2016, MNRAS, 463, 1117
Zolotov A. et al., 2012, ApJ, 761, 71

APPENDIX: FEEDBACK AT LOWER DM HALO MASSES

Uncertainties in the SFH determination may shift the peak of the SF to ∼1.2 Gyr younger ages than the true one and to artificially widen the age distribution (e.g. Aparicio et al. 2016). One might then wonder if it is possible that all the star formation activity that we have so far considered as taking place out to $z = 2$ was in reality confined to higher redshift, e.g. $z = 6$ (1 Gyr from the start of SF), i.e. to the pre-reionization era. At that time the DM halo would have been smaller and stellar feedback (coupled with the re-ionization UV background) could have been more efficient both in removing the gaseous component and in transforming a DM cusp into a core.

We deem this hypothesis unlikely for the kind of dwarf galaxies we are considering in this work: (1) the presence of a 'knee' in the [α/Fe] versus [Fe/H] trend for the almost purely old *fast* dwarf galaxies in the sample would suggest that chemical enrichment (and star formation) have been on-going for more than 1–2 Gyrs in these galaxies (see de Boer et al. 2012a for an age dating of the 'knee' in Sculptor). (2) Bovill & Ricotti (2011) show that it is unlikely that dwarf galaxies brighter than 1 million $L_{V,\odot}$ have formed more than 70 per cent of their stars by $z = 6$. By analyzing the SFH of Cetus, Tucana, LGS 3 and Phoenix (three of which are fainter than $L_{V,\odot} = 1 \times 10^6$) taking into account uncertainties in SFH determination, Aparicio et al. (2016) conclude that also these galaxies are unlikely to be reionization fossils. (3) From the work of Sawala et al. (2016a), it appears likely that dwarf galaxies as luminous as those considered here started and/or continued forming stars after re-ionization was completed.

Nonetheless, we will still revisit the calculations performed in the previous sections to understand the impact on our conclusion that stellar feedback cannot be the main reason for halting SF in most *fast* dwarfs; this also give us the opportunity to compare our predicted core sizes to those of Read et al. (2016), because the smaller halo masses predicted at $z = 6$ by the B14 and M13 relation are more similar to those considered in the hydrodynamical simulations by Read et al. (2016).

In order to determine the gravitational potential at $z = 6$, we follow the same procedure as in Section 4, but considering that at $z = 6$ the ratio between $M_{\rm vir}(z = 6)$ and $M_{\rm vir}(z = 0)$ according to Fakhouri et al. (2010) is about an ∼10 per cent for haloes in our mass regime (∼10^{10} $M_\odot$), and using the parameters of the equation (7) for $z = 6$ from Dutton & Macciò (2014). This results in DM halo masses ranging between 5×10^8 $M_\odot$ and 1.3×10^9 $M_\odot$. In this sense, the effect of making the calculations with the DM halo mass at $z = 6$ for the B14 and M13 AM relations is similar to choosing at $z = 2$ the AM relation by Behroozi et al. (2013) (which yields DM halo masses that range from ∼1.5×10^8 $M_\odot$ to ∼3×10^9 $M_\odot$ for our sample).

(i) Using the DM halo masses predicted at $z = 6$ with the B14 and M13 AM relations, we find that for $\epsilon_{\rm SN} = 0.1$ all the galaxies could remove their gas, including the *slow* types, which appears unrealistic since *slow* types have formed stars for practically a Hubble time and therefore they must have been able to hold on to a gas reservoir. We find that the maximum efficiency compatible with the slow dwarfs not losing their gas by $z = 6$ would be $\epsilon_{\rm SN} \lesssim 0.5$ per cent. Considering that $\epsilon_{\rm DM} \leq \epsilon_{\rm SN}$, this is compatible with the expected limits on the core radii of ∼ 2–5 kpc.
As mentioned above, the Behroozi et al. (2013) AM relation at $z = 2$ yields comparable DM halo masses to those from the B14 and M13 relation at $z = 6$. If we evolve back the DM halo masses with the Behroozi et al. (2013) AM relation at $z = 6$, the behaviour in terms of expected core radii would be even more catastrophic, which would set the efficiency then to even lower values.

(ii) The results from our simple calculations are in good agreement with the outcome of hydrodynamical simulations by Read et al. (2016), where the spatial scales relevant to follow the impact of individual SNe events are resolved. Let us for example focus on

the case of And XVI and Leo A, which according to our calculations have a DM halo mass of 5×10^8 M$_\odot$ and $\sim 1 \times 10^9$ M$_\odot$ at $z = 6$. These numbers are directly comparable to the 5×10^8 M$_\odot$ and $\sim 1 \times 10^9$ M$_\odot$ DM haloes in Read et al. (2016) (hereafter, medium and large R16 DM halo). Those simulated haloes formed a stellar component of $M_{\star,\mathrm{birth}} = 12.6 \times 10^5$ M$_\odot$ and 7.1×10^6 M$_\odot$, respectively, whose stellar feedback was found to have a coupling efficiency of 2 per cent, and created a core radius = 0.3 kpc in the former and 0.6 kpc in the latter, albeit after a long time (after 8 and 12 Gyr, respectively). For forming a DM core, what matters is the energy cumulatively injected into a DM halo of a given mass. The R16 conditions in terms of injected energy in their medium and large DM halo are comparable to our $M_{\star,\,z>2}$ of And XVI and Leo A if we assume $\epsilon_{\mathrm{DM}} = 0.01$ for the former and $\epsilon_{\mathrm{DM}} = 0.02$ for the latter; the resulting core radii are $\sim$0.1 kpc and $\sim$0.3 kpc, respectively. Considering the different IMF assumed and concentration parameter, the core sizes found in R16 hydrodynamical simulations and those predicted by our calculations are in good agreement. This lends support to the validity of our simplified approach.

(iii) The surroundings of the large LG spirals host a wealth of much fainter systems than 'classical' dwarf galaxies, commonly called UFDs. Some of these have SFHs consistent with having formed the great majority of their stars by $z = 6$ (e.g. Brown et al. 2014) or even being 'fossil' galaxies (e.g. Frebel, Simon & Kirby 2014). For these systems, e.g. of ancient stellar masses $\sim 10^4$–10^5 M$_\odot$, the energy balance calculated considering DM halo masses at $z = 6$, and requiring that the efficiency be less than 10–15 per cent, would result in the 10^5 M$_\odot$ systems being able to expel gas by internal feedback alone, while external effects would need to be invoked for the even fainter ones. In terms of core formation, it appears that the amount of available SN II feedback would be capable of forming a DM core larger than 0.1–0.2 kpc, i.e. of the order of the half-light radii observed for galactic systems of these stellar masses, already at extremely low efficiencies, between 1 and 10 per cent. The number of SN II produced is $\sim$280 and $\sim$2800 in the 10^4 and 10^5 cases, therefore stochastic sampling of the IMF in evaluating the produced internal feedback is probably not an issue at these stellar masses (see also e.g. Revaz et al. 2016). It remains to be assessed whether e.g. the assumptions of DM halo growth history and expected concentration at a given DM halo mass are appropriate also for the class of UFD systems.

This paper has been typeset from a TEX/LATEX file prepared by the author.